

Cover Page



Universiteit Leiden



The handle <http://hdl.handle.net/1887/58472> holds various files of this Leiden University dissertation.

**Author:** Witte, W.E.A. de

**Title:** Mechanistic modelling of drug target binding kinetics as determinant of the time course of drug action in vivo

**Issue Date:** 2017-12-19

**Chapter 4. *In vivo* target residence time and kinetic selectivity: the association rate constant as determinant.**

**Wilhelmus E.A. de Witte<sup>1</sup>, Meindert Danhof<sup>1</sup>, Piet H. van der Graaf<sup>1,2</sup>, Elizabeth C.M. de Lange<sup>1\*</sup>**

<sup>1</sup>Division of Pharmacology, Leiden Academic Centre for Drug Research, Leiden University, 2333 CC Leiden, The Netherlands

<sup>2</sup>Certara Quantitative Systems Pharmacology, Canterbury Innovation Centre, Canterbury CT2 7FG, United Kingdom

\* Correspondence: [ecmdelange@laccdr.leidenuniv.nl](mailto:ecmdelange@laccdr.leidenuniv.nl)

*Trends Pharmacol Sci* 2016;37(10):831–42

## Abstract

It is generally accepted that, in conjunction with pharmacokinetics, the first-order rate constant of target dissociation is a major determinant of the time course and duration of *in vivo* target occupancy. Here we show that the second-order rate constant of target association can be equally important. On the basis of the commonly used mathematical models for drug-target binding, it is shown that a high target association rate constant can increase the (local) concentration of the drug, which decreases the rate of decline of target occupancy. The increased drug concentration can also lead to increased off-target binding and decreased selectivity. Therefore, both the kinetics of target association and dissociation need to be taken into account in the selection of drug candidates with optimal pharmacodynamic properties.

## Glossary

**Endogenous ligand;** A compound that is naturally present in the body and functions by binding to a certain receptor.

**Endogenous competition;** Binding of an endogenous ligand to the same binding site as a drug.

**Kinetic selectivity;** Differential kinetics of a compound for binding to intended and unintended targets. Most often considered beneficial if the residence time on the intended target is longer than the residence time on the unintended targets

**Non-specific binding;** Drug binding to proteins, lipids or other materials that do not initiate signaling. Often unsaturated.

**Pharmacokinetics;** The combination of all processes that influence the concentration of a drug over time, including absorption, distribution, metabolism and excretion in all body compartments.

**Pharmacodynamics;** The combination of all processes that influence the relation between drug concentrations and drug effects.

**Residence time;** The average time each drug molecule remains bound to the target after the binding event, calculated as  $1/k_{\text{off}}$ .

**Rebinding;** The occurrence of multiple binding events during the dissociation phase, as a consequence of increasing unbound drug and target concentrations due to dissociation. Mostly used to describe the increased local drug concentration due to dissociation and limited diffusion near the drug target, for example in a synapse.

**Signal transduction;** The cascade of (cellular) reactions that is initiated by receptor activation and leads to the eventual effect.

**Target-Mediated Drug Disposition;** Extensive drug-target binding that influences the pharmacokinetic characteristics of a drug.

**Target occupancy;** The fraction of target that is bound to a drug or ligand molecule.

**Target Turnover;** Synthesis and degradation of a drug target leading to continuous regeneration of unbound target molecules.

## Optimisation of *in vivo* drug-target binding kinetics for drug discovery

To optimise the duration of drug action for its therapeutic use, developers have primarily focused on modification of pharmacokinetic parameters. However, an alternative approach is to optimise the duration of drug action by the modification of drug-target binding kinetics.

The target association and dissociation rate constants are important determinants of both the time course and the extent of drug effects, and their values can be measured in high-throughput *in vitro* systems. This has led to the inclusion of drug-target binding kinetics as a selection criterion in the evaluation of drug candidates in drug discovery [1,2].

Although drug-target binding kinetics can be optimised for different purposes regarding the magnitude and the kinetics of both wanted and unwanted drug effects [3–7], the most frequently proposed application is to prolong the duration of action by prolonging the **target occupancy** (see Glossary). Generally, the emphasis has been put on an increase of the target **residence time** through a reduction of the rate of target dissociation [8–10].

However, as drugs act in the human body, which is a complex and dynamic biological system, the duration of drug action is also influenced by other factors. These factors include the time course of the drug concentration (**pharmacokinetics**), the rates of synthesis and breakdown of the target molecule (**target turnover**), the concentrations of **endogenous ligands** competing for the same target, and the kinetics of the **signal transduction** [11].

Of these factors, the pharmacokinetics of the drug and the drug-target binding kinetics are the most frequently considered determinants of the time course of target occupancy. It is generally believed that the drug-target dissociation will only prolong target occupancy if it is slower than the rate of elimination of the drug [10].

While this rule of thumb offers a valuable approach to evaluate the role of drug-target binding kinetics, it does not account for all aspects of the complex interaction between the drug and its target. An important factor in this respect is that binding to the target can modify the local pharmacokinetics of the drug. In this way, binding of the drug to the target may lead to a decrease in the free drug concentration, while dissociation from the target may lead to an increase of the free drug concentration. This process is commonly referred to as “**target-mediated drug disposition**” or TMDD. The quantitative significance of this effect depends on the ratio of target-bound and unbound drug concentrations, which in turn depends on the target affinity of the drug and the concentration of the target in the biological system. Particularly for drugs with a high affinity for the target, target binding may reduce the elimination of the drug, as reflected in a long terminal phase in the decrease of the unbound plasma concentration, as has been demonstrated for warfarin and other drugs (Box 2) [12–19].

The influence of drug-target binding kinetics has not only been described for unbound drug concentrations in plasma, but also for unbound drug concentrations in the local environment of the target, such as a synapse or a cell membrane. In the local context, this interaction is commonly referred to as “diffusion-limited binding”, “**rebinding**” or drug-target binding from a “micro compartment” [20–24].

To understand the role of drug-target binding kinetics, others have analysed when binding equilibrium can be assumed in a TMDD model with target binding in plasma [17] and what the role of binding kinetics is when rebinding occurs [22]. Most recently, Vauquelin *et al.* demonstrated in a simulation study that both the drug-target association and dissociation rate constant have a similar impact on the duration of target occupancy if rebinding occurs [25]. However, an integrated analysis that indicates when binding kinetics are most relevant in a pharmacokinetic context, including tissue distribution, is currently missing.

Our aim here is to obtain such an integrated analysis. We firstly present an approximation to understand and visualize the role of drug-target binding kinetics if binding occurs in plasma. Subsequently, we expand this approximation to binding in a tissue. We obtain simple algebraic expressions to calculate when the drug-target dissociation rate is determining the duration of target occupancy for both binding in plasma and in tissues. Thus, we provide a connection of model-based insights from TMDD and rebinding models to predict the role of drug-target binding kinetics for drugs that bind to targets in the blood or in more peripheral tissues.

### **Drug-target binding *in vivo*: where does it happen?**

The commonly used mathematical models for drug-target binding were analysed in this study to yield a quantitative insight in the relative impact of drug-target binding kinetics and pharmacokinetics on the time course of target occupancy *in vivo*. The simplest model considers the situation where drug-target binding and elimination of the unbound drug occur simultaneously from the blood or from a tissue that is in fast equilibrium with the blood. This is schematically represented by Model 1 (Figure 1). The central compartment represents the blood and all organs that equilibrate quickly with the blood (see Box 1 for more information). Similar models have been used to describe binding to enzymes and binding to centrally expressed targets [26,27]. Note that absorption is not incorporated in this model and the dose is administered directly in the central compartment to represent intravenous dosing or very fast absorption.

Although drug-target binding from the blood is commonly seen for circulating enzymes or receptors on circulating cells, many drug targets are only expressed in specific tissues, such as the brain. For such targets, Model 2 (see Figure 1) might be more relevant. Model 2 is a common model for distribution into a specific tissue and binding to a drug target which is localised only in this tissue. This model has been used for a long time, for example to describe dopamine D<sub>2</sub> receptor binding in the human brain and  $\beta$ -Adrenergic receptor binding in the human heart [28,29]. The central compartment represents the blood and all organs that equilibrate quickly with the blood. Absorption is not incorporated in this model and the dose is given directly in the central compartment to represent intravenous dosing or very fast absorption.

### **Simultaneous elimination and drug-target binding: what's the difference?**

The influence of pharmacokinetics on the role of drug-target binding kinetics has been acknowledged previously. This influence has been summarized in the general paradigm that the rate of drug-target dissociation has to be slower than the rate of elimination of the unbound drug to prolong the duration of target occupancy. However, this general rule does not take into account the possible influence of drug-target binding on unbound drug concentration profiles. The influence of drug-target binding on the unbound drug concentration is known to be most pronounced for drugs with high affinities or high target concentrations (i.e. if the ratio of the target concentration and the affinity exceeds 1, see Box 2) [12]. As the interaction between pharmacokinetics and drug-target binding depends on the dissociation constant ( $K_D$ ), decreasing the drug-target dissociation rate constant ( $k_{off}$ ) or increasing the drug-target association rate constant ( $k_{on}$ ) will both have a similar impact on the unbound drug concentrations (Box 1 and Box 2). As a consequence, changing the  $k_{on}$  of a drug can have the same impact on the duration of target occupancy as changing the  $k_{off}$ . However, the impact of  $k_{on}$  and  $k_{off}$  on the initial increase of target occupancy might be different. The comparable impact on the duration of target occupancy of changing only  $k_{off}$  (left panels) or only  $k_{on}$  (right panels) is illustrated in Figure 2. The different rows in Figure 2 demonstrate that the impact of  $k_{on}$  and  $k_{off}$  on the duration of target occupancy depends on the target concentration and the elimination rate constant  $k_{el}$ : In the first row, where the target concentration is 10 nM, the impact of  $k_{on}$  and  $k_{off}$  is very similar, but in the second row, where the target concentration has changed to 1 nM, the impact of  $k_{on}$  and  $k_{off}$  is different, as can be seen most clearly for the yellow and the blue line. In the bottom row, where the target concentration stays 1 nM and the elimination rate constant changes from 1 to 0.1 h<sup>-1</sup>, the impact of  $k_{on}$  and  $k_{off}$  on the duration of target occupancy is again similar.

### Box 1. Drug-target binding in compartmental models.

Compartmental models are the most common form of mathematical models in pharmacology. In these models, the different locations and states in which the drug can occur are lumped into one or more compartments. Differential equations are used to describe the time profile in each compartment (see Supplemental Information S1 for the differential equations of Model 1 and Model 2). The underlying assumptions of a compartmental description of drug-target binding are the following:

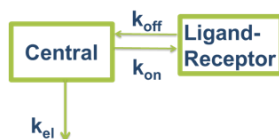
1. *Homogeneity within each compartment: Although the represented biological systems are clearly non-homogeneous, the assumption of homogeneity can be used if equilibration within each compartment is sufficiently fast.*
2. *Drug-target binding occurs in the unbound drug compartment: As the drug target has to reside in the same location as the unbound drug to enable drug-target binding, the volume of the ligand-receptor compartment and the volume of the unbound drug compartment that drives the drug-target binding (i.e. the tissue compartment for Model 2) are assumed to be the same.*

Model 1 connects the drug concentration to the target binding according to the law of mass action. The law of mass action states that the rate of elementary (single-step) chemical reactions is proportional to the product of the concentrations of the reactants. This results in the familiar equations that describe the drug-target association rate as the product of the drug-target association rate constant  $k_{on}$ , the unbound target concentration  $[R]$  and the unbound ligand concentration  $[L]$ , while the drug-target dissociation rate is the product of the dissociation rate constant  $k_{off}$  and the bound ligand concentration  $[LR]$ . As the drug-target association and dissociation rates are equal in equilibrium, this leads to the common equilibrium equation for the dissociation constant  $K_D$ :

$$K_D = \frac{[L] \cdot [R]}{[LR]} = \frac{k_{off}}{k_{on}}$$

In a closed system (without drug or target elimination) with a low target concentration (as in most in vitro binding experiments)  $[L]$  can be assumed to be constant and much larger than  $[R]$ . This has led to analytical expressions that describe the drug-target binding profile in vitro, such as published by Motulsky and Mahan [39]. For the in vivo situation,  $[L]$  is not constant, because high target concentrations can lead to depletion of the ligand upon binding, and because of drug elimination. Thus, in vivo drug-target binding cannot be simplified in the same way as in vitro drug-target binding.

## Model 1



## Model 2

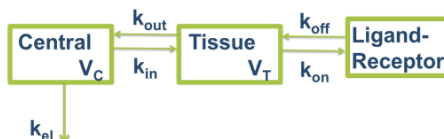


Figure 1. Schematic representation of the two models that are used in this study. Model 1 describes drug-target binding in the central compartment (representing blood and quickly equilibrating tissues) with the second-order association rate constant  $k_{on}$  and the first order dissociation rate constant  $k_{off}$ . Elimination of the drug from the body (by excretion or metabolism) is described by the first order rate constant  $k_{el}$ . Model 2 describes drug-target binding from a tissue, and distribution into and out of the tissue is described by the first-order rate constants  $k_{in}$  and  $k_{out}$ , respectively. The differential equations of Model 1 and 2 can be found in Supplemental Information S1.

### Box 2. Target-Mediated Drug Disposition.

To describe the influence of extensive drug-target binding on the pharmacokinetic profile of the drug, the term “Target-Mediated Drug Disposition” (TMDD) was introduced by Levy et al. in 1994[35]. Extensive target binding occurs mainly when the ratio of total target concentration/dissociation constant  $K_D$  is larger than 1, as a consequence of the law of mass action. For example, if the unbound concentration of a drug in binding equilibrium is 5 nM, the total target concentration is 50 nM and the  $K_D$  is 5 nM, 50 % of the target will be occupied, which corresponds to 25 nM. This means that the concentration of the bound drug is five times larger than the concentration of the unbound drug. As most drugs can only be eliminated if they are unbound, this extensive target binding leads to a slower elimination of drug from the body, compared to the situation without extensive target binding. This extensive target binding decreases if the target becomes saturated. If the drug concentration is increased from 5 to 500 nM for the example of a target concentration of 50 nM and a  $K_D$  of 5 nM, the equilibrium occupancy becomes 99%, corresponding to a target-bound drug concentration of 50 nM. This means that the concentration of bound drug is now ten times smaller than the concentration of the unbound drug. The impact of extensive target binding on free drug concentrations in plasma is most apparent if the average target concentration is high in the whole body. This has led to the frequent application of TMDD models to describe the plasma concentration profile of antibodies, as they often bind with high affinity to centrally expressed targets [14]. Since the degradation/internalization of target-bound antibodies often contributes significantly to the elimination of the total amount of antibody, TMDD models often incorporate these processes [16]. If extensive target binding only occurs locally and not in the whole body, this can lead to a longer effect compared to what is expected on basis of unbound plasma concentrations.

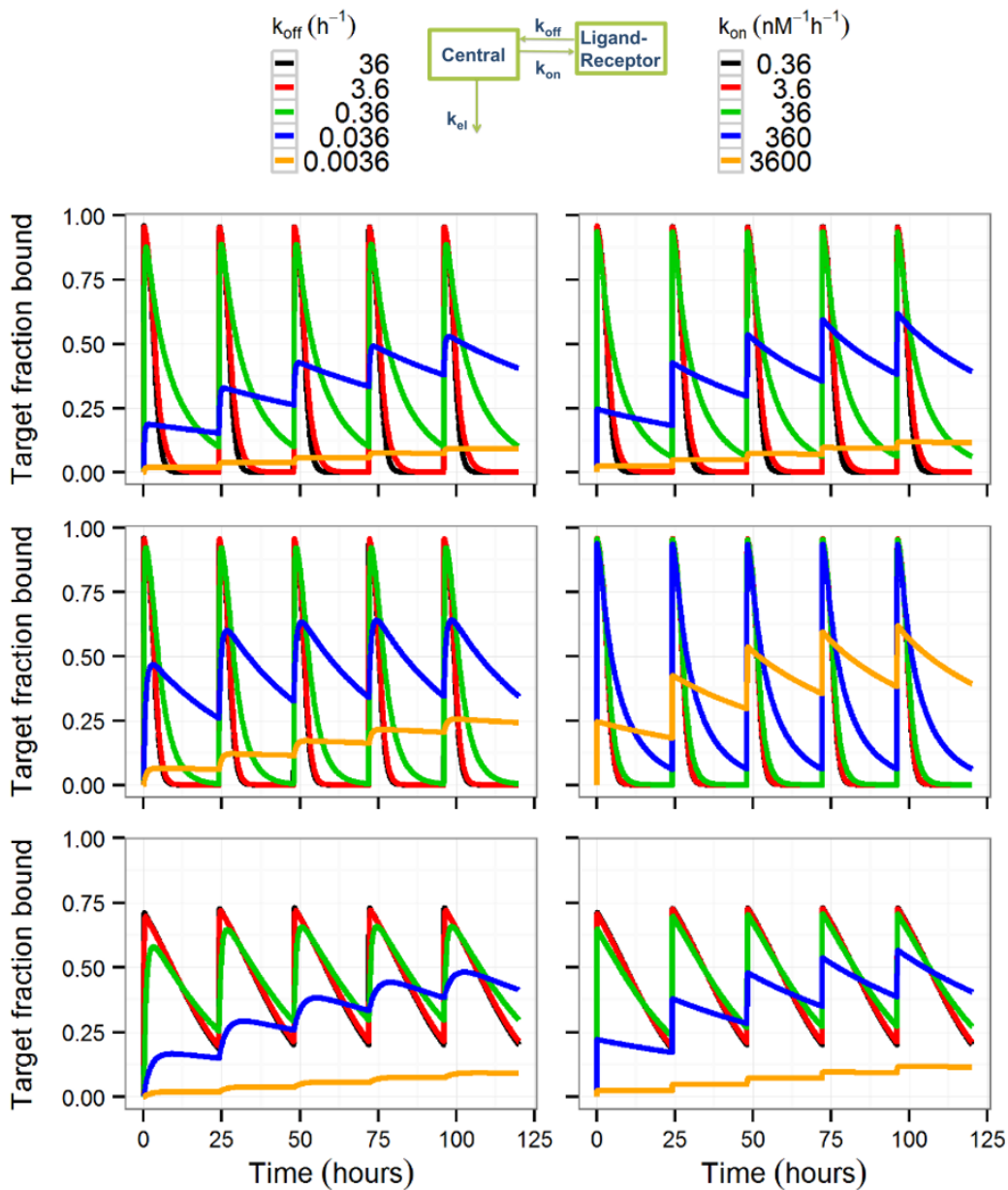


Figure 2. Simulation of the target fraction bound for drug-target binding in the blood (Model 1). The simulated affinities are increased by changing either the dissociation rate constant  $k_{off}$  (left panels) or the association rate constant  $k_{on}$  (right panels). The  $k_{on}$  was  $0.36 \text{ nM}^{-1}\text{h}^{-1}$  for all lines in the left panels and the  $k_{off}$  was  $36 \text{ h}^{-1}$  for all lines in the right panels. The initial concentration is  $25 \cdot K_D$  for the top and middle row and  $2.5 \cdot K_D$  for the bottom row, to achieve similar maximal occupancies in all panels.  $K_D$  is the drug-target dissociation equilibrium constant and  $k_{el}$  is the drug elimination rate constant.  $[R_{tot}]$  = total target concentration. Top row:  $[R_{tot}] = 10 \text{ nM}$ ,  $k_{el} 1 \text{ h}^{-1}$ , middle row:  $[R_{tot}] = 1 \text{ nM}$ ,  $k_{el} 1 \text{ h}^{-1}$ , bottom row:  $[R_{tot}] = 1 \text{ nM}$ ,  $k_{el} 0.1 \text{ h}^{-1}$ .

The influence of pharmacokinetics, target concentration, and affinity on drug-target binding kinetics requires simultaneous analysis of the influence of all parameters. To focus on the duration of target



occupancy, we derived an approximation of the decrease of target occupancy after its maximal value. This decrease of target occupancy is described here as the derivative of the target fraction bound (BF) vs. time curve. As the decrease of target occupancy often follows an exponential decline, the derivative is calculated for the semi logarithmic target fraction bound (BF) vs. time curve, where the target fraction bound is on the logarithmic axis. The derivative of the semi logarithmic target fraction bound (BF) vs. time curve, called  $\lambda_{TO}$  here, is not always constant over time as it depends on the saturation of drug-target binding: If the drug concentration is much higher than the affinity and all target molecules are bound to the drug, a relatively small proportion of the drug is bound to the target and the elimination of the drug is not limited by target binding. Also, if target binding is saturated and the unbound drug concentration decreases with a certain percentage, the target fraction bound decreases much less than that percentage. However, a fractional decrease in the unbound drug concentration will result in a similar decrease in the target fraction bound if the target fraction bound is low and binding is not saturated. As an example, if the unbound drug concentration decreases 90% from 500 to 50 nM for a drug with a  $K_D$  of 5.0 nM, the corresponding equilibrium bound fraction decreases 7%: from 0.99 to 0.91. If the unbound drug concentration decreases 90% from 50 to 0.50 nM for a drug with a  $K_D$  of 5.0 nM, the corresponding equilibrium bound fraction decreases 82%: from 0.50 to 0.091, (see also box 2 and Supplemental Information S2). As the derivative of the semi logarithmic target fraction bound (BF) vs. time curve,  $\lambda_{TO}$ , depends on the saturation of drug-target binding, it can be expressed as a function of the target fraction bound:  $\lambda_{TO}(BF)$ .

Our approximation is based on the assumption that the process that results in the slowest decrease of target occupancy (elimination or dissociation) will determine the decrease of target occupancy as rate-limiting step. To predict which of these processes is the rate-limiting step in the decrease of target occupancy, one needs to take into account that only elimination of the unbound drug occurs, and elimination is thus limited by drug-target binding. Moreover, incorporation of the influence of drug-target target saturation on the relationship between the decline of unbound and target-bound drug concentrations is required. As demonstrated in Supplemental Information S2, the derivative of the semi logarithmic target fraction bound (BF) vs. time curve, as function of BF,  $\lambda_{TO}(BF)$ , can be approximated on this basis. The resulting approximation of  $\lambda_{TO}(BF)$  for the physiological range of parameter values for Model 1 reveals 3 different situations for the influence of drug-target binding kinetics on the duration of target occupancy:

- 1) Only the  $k_{off}$  determines the duration of target occupancy. This is the case if drug-target dissociation is the rate-limiting step for the decrease of the target occupancy.
- 2) Both  $k_{off}$  and  $k_{on}$  influence the duration of target occupancy equally. The duration of target occupancy is determined by the dissociation constant  $K_D$ , the elimination rate constant  $k_{el}$ , and the total target concentration  $[R_{tot}]$ .
- 3) Only the elimination rate constant  $k_{el}$  determines the duration of target occupancy.

Which of these situations applies for a specific drug depends on the value of  $k_{on}$  and  $k_{off}$ , but also on the target concentration and the pharmacokinetic parameters. The situation where drug-target dissociation is rate limiting and  $k_{off}$  the only determinant for the decrease of target occupancy requires both a low value for  $k_{on}$  and  $k_{off}$ . On basis of our approximation, we could identify a constant for the value of  $k_{off}$  and  $k_{on}$  that results in drug elimination as the rate-limiting step in the decrease of target occupancy. The constants that approximate the threshold value of  $k_{on}$  and  $k_{off}$  for the rate-limiting step,  $K_{RLon}$  and  $K_{RLOff}(BF)$ , are given by Equation 1 and 2 (which are derived as equation S25 and S26). It should be noted that the  $K_{RLon}$  is independent of target saturation while  $K_{RLOff}(BF)$  is dependent on target saturation and thus given as function of the target fraction bound (BF).

#### Equation 1

$$K_{RLon} = \frac{k_{el}}{k_{on} \cdot [R_{tot}]}$$

### Equation 2

$$K_{RLoff}(BF) = \frac{k_{el} \cdot (1 - BF)}{k_{off}}$$

If  $K_{RLon}$  and  $K_{RLoff}(BF)$  are both greater than 1, dissociation is the rate-limiting step in the decrease of target occupancy, which is then determined by  $k_{off}$ . If either of these constants is smaller than 1, elimination is the rate-limiting step in the decrease of target occupancy.

If elimination is the rate-limiting step in the decrease of target occupancy, the decrease rate can be either determined by the  $k_{el}$  alone, or by  $k_{el}$ ,  $k_{on}$  and  $k_{off}$ . The maximal value of  $k_{off}$  that leads to an elimination rate that is significantly influenced by  $k_{el}$ ,  $k_{off}$  and  $k_{on}$  is given in Equation 3 (derived as equation S28).

### Equation 3

$$k_{off} = k_{on} \cdot [R_{tot}] \cdot (1 - BF)$$

Equations 1-3 provide the basis to identify which of the situations regarding the influence of drug-target binding kinetics on the duration of target occupancy applies, as visualised in Figure 3.

The analysis of Model 1 as presented in Figure 3 provides several general insights for drug discovery:

- 1) Increasing the  $k_{on}$  can increase the duration of target occupancy (indicated by the changing color in the horizontal direction), even if the  $k_{off}$  is higher than the  $k_{el}$ .
- 2) If the  $k_{on}$  or the  $k_{off}$  is sufficiently high to result in a  $K_{RLon}$  or  $K_{RLoff}(BF) > 1$ , decreasing the  $k_{off}$  has the same impact on the duration of target occupancy as increasing the  $k_{on}$  (indicated by the diagonal color bands in the lower right corner).
- 3) If both the  $k_{off}$  and the  $k_{on}$  value are sufficiently low to make both  $K_{RLon}$  and  $K_{RLoff}(BF) < 1$ , drug-target dissociation is rate-limiting and  $k_{off}$  determines the duration of target occupancy (as indicated by the horizontal color bands in the lower left corner). A rate-limiting drug-target dissociation is required to obtain a slower decline of target occupancy than expected on basis of the unbound drug concentration and the drug-target affinity. This means that only a combination of a low  $k_{off}$  and a low  $k_{on}$  could lead to longer binding to the intended than to the unintended target (which also requires a lower dissociation rate from the intended compared to the dissociation rate from the unintended target, i.e. **kinetic selectivity**) [1,30].

Model 1 applies to drugs which have their target in the blood or in a tissue that equilibrates rapidly with blood. Mainly targets that are expressed in the blood, such as circulating enzymes (HSP90, Factor X) have target concentrations higher or similar to the highest target concentration of 20 nM in Figure 3 [26,31].

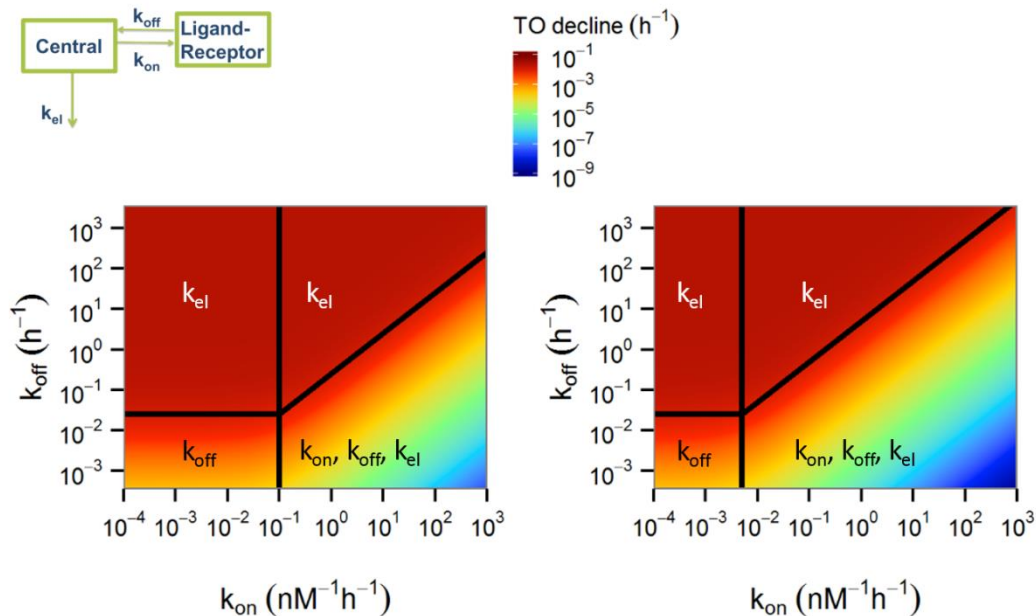


Figure 3. Approximation of the decline in target occupancy using Model 1. The total target concentration is 1 nM (left panel) and 20 nM (right panel), the elimination rate constant is 0.1/h and the target fraction bound is 0.75, to represent a clinically relevant degree of target occupancy. Colors represent the decrease of target occupancy ( $\lambda_{TO}(BF)$ ) as calculated according to Supplemental Information S2 (Equation S19). The vertical line is given for  $K_{RLon} = 1$  (see Equation 1), the horizontal line is given by  $K_{RLoff}(BF) = 1$  (see Equation 2) and the diagonal line is given by Equation 3. In these equations,  $k_{el}$  is the elimination rate constant,  $[R_{tot}]$  is total target concentration and BF is the bound fraction of the target. The annotations indicate which parameters influence the decrease in target occupancy in the corresponding segment of the plot. This figure is an approximation of Model 1 (insert) (Supplemental Information S2).

### Is the impact of drug-target binding kinetics different for target binding in a tissue?

To expand our understanding of drug-target binding, a similar analysis was performed for drugs that bind only in a specific tissue, similarly as was done for drug-target binding from the blood. The results of this analysis can be found in Supplemental Information S3. One of the main differences with the analysis for Model 1 is that the drug distribution from the tissue to the central compartment can be rate limiting for Model 2. A high value of  $k_{on}$  still leads to an equal impact of  $k_{on}$  and  $k_{off}$  on the decline of target occupancy in the same way as for Model 1 if drug distribution out of the tissue is rate-limiting, but this is not necessarily reflected in the unbound plasma concentration versus time profile. Moreover, rate-limiting elimination can similarly influence the duration of target occupancy due to extensive target binding, but this occurs only at high target concentrations in the tissue, as the fraction of the total amount of drug in the body that is bound to the target decreases for decreasing volumes of the drug-target binding tissue.

To understand what our analysis means for drug discovery, our equations have been applied to a combination of common pharmacokinetic parameters (Figure 4, key figure). A small literature survey was performed to find a common value for the total tissue target concentration. The target concentration for common targets such as  $\mu$ -opioid [23], adenosine [32], dopamine D2 [28], GABA [33], 5-HT [34], and Vitamin K epoxide reductase [35] varied between 2 [34] and 2000 [35] nM, with most values in the range between

10 and 100 nM. As can be seen in Figure 4, our analysis reveals a very similar influence of the drug-target binding kinetics for drug-target binding in tissue compared to drug-target binding in the blood (Figure 4).

To investigate how the combination of  $k_{on}$  and  $k_{off}$  values of drug discovery compounds relate to the expected determinants of the duration of target occupancy, all compounds from the K4DD (kinetics for drug discovery <http://www.k4dd.eu>) consortium database were included in Figure 4. This K4DD database is brought together by both industry and academia and consists of *in vitro* binding kinetics measurements of small molecule drug discovery compounds on different targets, including kinases and GPCRs. We will refer to this data set as the “discovery dataset”.

Moreover, a literature dataset of compounds with known drug-target binding kinetics which were developed into drugs or drug candidates, as published by Dahl and Akerud [10], was also included in Figure 4. Below, we will refer to this dataset as the “candidate dataset”. The data in Figure 4 show that the majority of compounds from both datasets have high  $k_{on}$  values for the common pharmacokinetic parameters and target concentration and would be expected to have an equal influence of both  $k_{on}$  and  $k_{off}$  on the duration of target occupancy. Moreover, as the drug distribution is rate limiting for the decline of target occupancy for a high value of  $k_{on}$  and the given pharmacokinetic parameters and target concentration in Figure 4, binding equilibrium will be reached and no kinetic selectivity is expected over unintended targets that are located in the same tissue as the intended target. Interestingly, comparison of the discovery and the candidate dataset shows a similar distribution of  $k_{on}$  values in both datasets, but a distribution of  $k_{off}$  values which is approximately one order of magnitude lower for the candidate dataset. The differential distribution for  $k_{off}$  but not for  $k_{on}$  in these datasets can have multiple explanations. As indicated by others,  $k_{on}$  is often less sensitive to chemical modifications of similar compounds or for biological modifications of the target compared to  $k_{off}$  [36]. Also, the selection of drug (candidates) was based on the availability of drug-target binding kinetics, which could lead to a biased dataset for compounds where the drug-target binding kinetics plays a more significant role. Moreover, achieving a high affinity in drug discovery and development by changing the  $k_{on}$  is limited by the diffusion-limited maximal value of  $k_{on}$ , whereas the  $k_{off}$  has no theoretical minimum until irreversible binding is reached [37].

The similar values for  $k_{on}$  in both datasets correspond with our finding that an increasing  $k_{on}$  can increase the duration of target occupancy but at the cost of increasing the (local) drug concentrations, which can result in increased side effects. Moreover, the observation of lower  $k_{off}$  values in the candidate dataset indicates that a low  $k_{off}$  value might contribute to successful drug development. Dahl and Akerud observed that the drug-target dissociation for most compounds in the candidate dataset is slower than the plasma elimination, which means in their analysis that the elimination rate determines the duration of target occupancy (assuming there is no rebinding). In our analysis, the high  $k_{on}$  values in the candidate and in the discovery dataset result in a decline of target occupancy that is influenced by the elimination rate constant and the binding affinity and that the resultant decline of target occupancy can be slower than the elimination and the dissociation rates.

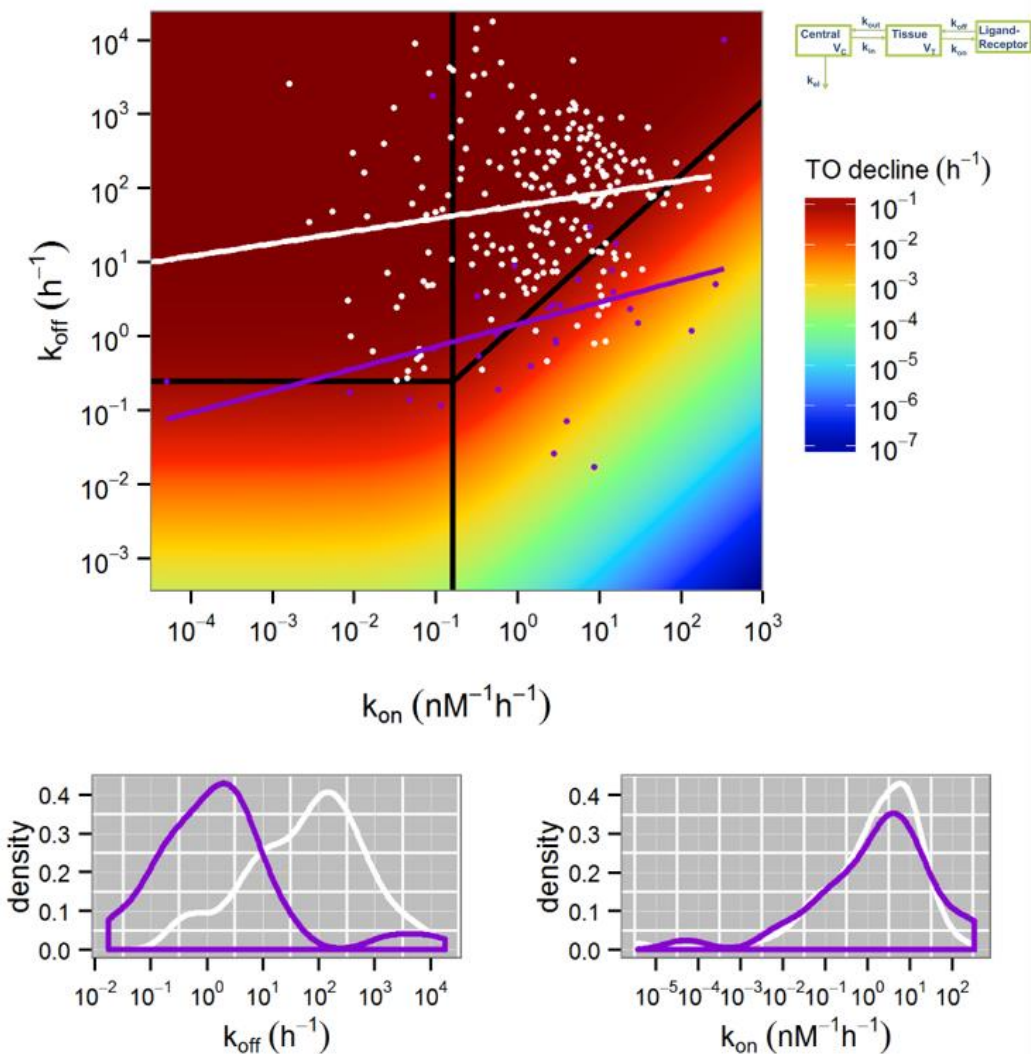


Figure 4. Calculated duration of target occupancy for drug-target binding in a tissue (Model 2). Top panel: Relation between drug-target binding kinetics and the duration of target occupancy for binding in tissue. The points and their linear regressions provide an overview of the distribution of binding kinetics measurements of all compounds in the drug discovery compound database of the K4DD consortium (white) or the drug (candidate) dataset from the review published by Dahl and Akerud (purple). The colors and black lines depend on the pharmacokinetic parameters according to equation S35 in Supplemental Information S3 and are based on Model 2 (insert) with the following parameter values:  $[R_{tot}] = 50 \text{ nM}$ ,  $k_{el} = 0.5/\text{hr}$ ,  $k_{in} = 0.2/\text{hr}$ ,  $V_c = 40 \text{ L}$ ,  $V_T = 1 \text{ L}$ ,  $BF = 0.5$ .  $[R_{tot}]$  is the total target concentration,  $k_{el}$  is the elimination rate constant,  $k_{in}$  is the brain to plasma distribution rate constant,  $V_c$  is the volume of the central compartment,  $V_T$  is the volume of the tissue and  $BF$  is the bound fraction of the target. Bottom panels: distribution of the dissociation (left) and association (right) rate constants of both datasets with the corresponding colors in the top panel. The distribution of the parameter values of each dataset is plotted as the estimated probability density function.

## Optimising drug-target binding kinetics: to what end?

Both for drug-target binding in plasma and in tissue, our analysis indicates that high  $k_{on}$  values can decrease the target occupancy decline below the elimination and dissociation rates. However, this increased duration of target occupancy is caused by increased (local) drug concentrations unless both  $k_{off}$  and  $k_{on}$  are low. This means that the optimal value for  $k_{on}$  depends on the target, the drug class and the drug-specific pharmacokinetic, **pharmacodynamic** and toxicity processes.

If an increased duration of target occupancy is desired, this can be achieved by both increasing the  $k_{on}$  or by decreasing the  $k_{off}$ . If the  $k_{on}$  is high enough,  $k_{on}$  and  $k_{off}$  have the same impact on the duration of target occupancy (Figure 2, top and bottom row), but not on the initial increase rate of target occupancy after dosing (Figure 2, bottom row). Moreover, a high value of  $k_{on}$  will lead to increased local drug concentrations and a rate-limiting role for the pharmacokinetics, which can result in increased off-target binding and decreased selectivity. How drug target binding can influence only local drug concentrations is illustrated by our simulations for diprenorphine (Supplemental Information S4 and S5).

Our analysis is based on a simplification of the complex biological system that determines the duration of target occupancy, see Outstanding Questions. Three important factors that can play a role in the kinetics of target occupancy are **non-specific binding**, **endogenous competition** and **target turnover**. Non-specific binding could influence the relevance of our analysis as a high percentage of non-specific binding could mean that the impact of specific binding on drug concentrations decreases for drugs with extensive non-specific binding. Also, the presence of an endogenous ligand that competes for binding to the drug target will reduce the number of available target molecules and thus decrease the impact of drug-target binding. Moreover, the synthesis and degradation of the target and drug-target complex can increase the decline of target occupancy and thus decrease the impact of drug-target binding. However, our analysis provides a quantitative improvement of the commonly used consideration that only a drug-target dissociation rate lower than the plasma elimination rate can influence the duration of target occupancy [10,36].

Apart from these complications, the validity of our findings depends on the validity of our assumptions and mathematical method. However, mathematical and experimental findings that explored the interaction between local concentrations in the target vicinity and drug-target binding (“rebinding”) also pointed towards the importance of  $k_{on}$  in similar equations [20–22,38]. Moreover, published [3H] diprenorphine plasma and brain concentrations were fitted with Model 2 for this study, and subsequent simulations with varying drug-target binding kinetics revealed an equal impact of  $k_{on}$  and  $k_{off}$  on the target occupancy profile over time, as expected from our analysis (Supplemental Information S4 and S5). Supplemental Information S4 supports the relevance of the analysed model, Model 2, as it is able to describe the experimental data of diprenorphine plasma and brain concentration. Supplemental Information S5 supports the necessary assumptions that were made to analyse Model 2, as the role of binding kinetics in the full model corresponds with the predicted role of binding kinetics from our approximation. Finally, comparison of approximated and simulated target occupancy vs. time derivatives indicated a high accuracy of our approximation and a high relevance of our assumptions, except for the combination of low association, dissociation and elimination rate constants with low target concentrations (Supplemental Information S6). Altogether, this supports the relevance and validity of our analysis.

To enable the rational use of drug-target binding kinetics in drug discovery, the whole kinetic context between drug dosing and effect should be taken into account. The algebraic equations as presented in this study provide a first step to integrate and understand both pharmacokinetics and drug-target binding kinetics. If the pharmacokinetic parameters are unknown, commonly observed values can be used, as demonstrated in Figure 4. If more detailed information is required on both the duration and the extent of target occupancy, simulations of the compartmental models can be performed easily.

## Concluding Remarks

Comprehensive analysis of the commonly used models for drug-target binding reveals that high drug-target association rate constants result in longer target occupancy than expected on basis of the drug-target dissociation and the drug elimination rate constants. The  $k_{on}$  value that separates high and low values of  $k_{on}$  increases with increasing target concentration and with decreasing drug elimination and distribution rate constants and can be calculated algebraically. High values of  $k_{on}$ , for common pharmacokinetic parameter values, are observed frequently for both drug discovery and drug (candidate) compounds and result in an equal impact of both  $k_{on}$  and  $k_{off}$  on the duration of target occupancy. However, these high  $k_{on}$  values can lead to more off-target toxicity. Comparison of drug discovery and drug (candidate) compounds shows similar distributions of  $k_{on}$  while  $k_{off}$  is approximately one order of magnitude smaller for the drug (candidate) compounds.

The target occupancy versus time profile can only be predicted if the target concentration and the rate constants of drug binding, elimination and distribution are taken into account, which often results in an equal impact of  $k_{on}$  and  $k_{off}$  on the duration of target occupancy.

Our findings demonstrate that optimizing the drug discovery requires mechanistic knowledge of the intended mechanism of action, including the in vivo concentration of the drug target. Moreover, the role of the drug-target association rate constant ( $k_{on}$ ) should be taken into account in the optimization of the duration of drug effects. Although this study does not include all relevant processes that can influence the duration of drug effects following administration of a drug (see Outstanding Questions box), the presented integration of target binding and pharmacokinetics is an important step towards a more rational selection of drug candidates.

## Acknowledgements

The authors wish to thank professor L. A. Peletier for critically reading the manuscript and providing useful feedback.

The authors are part of the K4DD (Kinetics for Drug Discovery) consortium which is supported by the Innovative Medicines Initiative Joint Undertaking (IMI JU) under grant agreement no 115366. The IMI JU is a project supported by the European Union's Seventh Framework Programme (FP7/2007–2013) and the European Federation of Pharmaceutical Industries and Associations (EFPIA).

## References

1. Copeland RA, Pompliano DL, Meek TD. Drug-target residence time and its implications for lead optimization. *Nat Rev Drug Discov* 2006;5(9):730–9
2. Shiau AK, Massari ME, Ozbal CC. Back to basics: label-free technologies for small molecule screening. *Comb Chem High Throughput Screen* 2008;11(3):231–7
3. Swinney DC. The role of binding kinetics in therapeutically useful drug action. *Curr Opin Drug Discov Devel* 2009;12(1):31–9
4. Langlois X, Megens A, Lavreysen H, et al. Pharmacology of JNJ-37822681, a specific and fast-dissociating D2 antagonist for the treatment of schizophrenia. *J Pharmacol Exp Ther* 2012;342(1):91–105
5. Kapur S, Seeman P. Does Fast Dissociation From the Dopamine D 2 Receptor Explain the Action of Atypical Antipsychotics?: A New Hypothesis. *Am J Psychiatry* 2001;158(3):360–9
6. Sykes DA, Dowling MR, Charlton SJ. Exploring the mechanism of agonist efficacy: a relationship between efficacy and agonist dissociation rate at the muscarinic M3 receptor. *Mol Pharmacol* 2009;76(3):543–51
7. Sykes DA, Riddy DM, Stamp C, et al. Investigating the molecular mechanisms through which FTY720-P causes persistent S1P1 receptor internalization. *Br J Pharmacol* 2014;171(21):4797–807
8. Copeland RA. The dynamics of drug-target interactions: drug-target residence time and its impact on efficacy and safety. *Expert Opin Drug Discov* 2010;5(4):305–10
9. Guo D, Hillger JM, Ilzerman AP, et al. Drug-target residence time - a case for G protein-coupled receptors. *Med Res Rev* 2014;34(4):856–92
10. Dahl G, Akerud T. Pharmacokinetics and the drug-target residence time concept. *Drug Discov Today* 2013;18(15–16):697–707
11. de Witte WEA, Wong YC, Nederpelt I, et al. Mechanistic models enable the rational use of in vitro drug-target binding kinetics for better drug effects in patients. *Expert Opin Drug Discov* 2016;11(1):45–63
12. Wagner JG. A new generalized nonlinear pharmacokinetic model and its implications. In: Wagner JG, editor. *Biopharmaceutics and Relevant Pharmacokinetics* Hamilton, IL; 1971. p. 302–17
13. Mager DE, Jusko WJ. General pharmacokinetic model for drugs exhibiting target-mediated drug disposition. *J Pharmacokinet Pharmacodyn* 2001;28(6):507–32
14. Dua P, Hawkins E, van der Graaf P. A Tutorial on Target-Mediated Drug Disposition (TMDD) Models. *CPT Pharmacometrics Syst Pharmacol* 2015;4(6):324–37
15. Mager DE, Krzyzanski W. Quasi-Equilibrium Pharmacokinetic Model for Drugs Exhibiting Target-Mediated Drug Disposition. *Pharm Res* 2005;22(10):1589–96
16. Peletier LA, Gabrielsson J. Dynamics of target-mediated drug disposition: characteristic profiles and parameter identification. *J Pharmacokinet Pharmacodyn* 2012;39(5):429–51
17. Ma P. Theoretical considerations of target-mediated drug disposition models: simplifications and approximations. *Pharm Res* 2012;29(3):866–82
18. Abraham AK, Krzyzanski W, Mager DE. Partial derivative-based sensitivity analysis of models describing target-mediated drug disposition. *AAPS J* 2007;9(2):E181-9
19. Aston PJ, Derks G, Raji A, et al. Mathematical analysis of the pharmacokinetic-pharmacodynamic (PKPD) behaviour of monoclonal antibodies: Predicting in vivo potency. *J Theor Biol* 2011;281(1):113–21
20. Coombs D, Goldstein B. Effects of the geometry of the immunological synapse on the delivery of effector molecules. *Biophys J* 2004;87(4):2215–20
21. DeLisi C. The biophysics of ligand-receptor interactions. *Quarterly Rev Biophys* 1980;13(2):201–30
22. Vauquelin G. Rebinding : or why drugs may act longer in vivo than expected from their in vitro target residence time. *Expert Opin Drug Discov* 2010;5(10):927–41
23. Perry DC, Mullis KB, Oie S, et al. Opiate antagonist receptor binding in vivo: evidence for a new receptor binding model. *Brain Res* 1980;199(1):49–61
24. Szczuka A, Wennerberg M, Packeu A, et al. Molecular mechanisms for the persistent bronchodilatory effect of the beta 2-adrenoceptor agonist salmeterol. *Br J Pharmacol* 2009;158(1):183–94
25. Vauquelin G. Impact of target binding kinetics on in vivo drug efficacy: koff, kon and rebinding. [Internet]. *British Journal of Pharmacology*. 2016. Epub ahead of print p
26. Yamazaki S, Shen Z, Jiang Y, et al. Application of target-mediated drug disposition model to small molecule heat shock protein 90 inhibitors. *Drug Metab Dispos* 2013;41(6):1285–94
27. Francis RJ, Brown AN, Kler L, et al. Pharmacokinetics of the converting enzyme inhibitor cilazapril in normal volunteers and the relationship to enzyme inhibition: Development of a mathematical model. *J Cardiovasc Pharmacol* 1987;9(1):32–8
28. Farde L, Eriksson L, Blomquist G, et al. Kinetic Analysis of Central [ IIC ] Raclopride Binding to D2-Dopamine Receptors Studied by PET-A Comparison to the Equilibrium Analysis. *J Cereb Blood Flow Metab* 1989;9(5):696–708



29. Doze P, Elsinga PH, van Waarde A, et al. Quantification of  $\beta$ -adrenoceptor density in the human heart with ( S )-[ 11 C]CGP 12388 and a tracer kinetic model. *Eur J Nucl Med Mol Imaging* 2002;29(3):295–304
30. Guo D, Dijksteel GS, Van Duijl T, et al. Equilibrium and kinetic selectivity profiling on the human adenosine receptors. *Biochem Pharmacol* 2016;105:34–41
31. Fair DS, Edgington TS. Heterogeneity of hereditary and acquired factor X deficiencies by combined immunochemical and functional analyses. *Br J Haematol* 1985;59(2):235–48
32. Bruns RF, Daly JW, Snyder SH. Adenosine receptors in brain membranes: Binding of N6-cyclohexyl[3H]adenosine and 1,3-diethyl-8-[3H]phenylxanthine. *Proc Natl Acad Sci USA* 1980;77(9):5547–51
33. Millet P, Graf C, Moulin M, et al. SPECT quantification of benzodiazepine receptor concentration using a dual-ligand approach. *J Nucl Med* 2006;47(5):783–92
34. Costes N, Merlet I, Zimmer L, et al. Modeling [18 F]MPPF Positron Emission Tomography Kinetics for the Determination of 5-Hydroxytryptamine(1A) Receptor Concentration With Multiinjection. *J Cereb Blood Flow Metab* 2002;22(6):753–65
35. Levy G. Pharmacologic target-mediated drug disposition. *Clin Pharmacol Ther* 1994;56(3):248–52
36. Copeland RA. The drug-target residence time model: a 10-year retrospective. *Nat Rev Drug Discov* 2016;15(2):87–95
37. Zhou G-Q, Zhong W-Z. Diffusion-Controlled Reactions of Enzymes. A Comparison between Chou’s Model and Alberty-Hammes-Eigen’s Model. *Eur J Biochem* 1982;387(2–3):383–7
38. Goldstein B, Dembo M. Approximating the effects of diffusion on reversible reactions at the cell surface: ligand-receptor kinetics. *Biophys J* 1995;68(4):1222–30
39. Motulsky HJ, Mahan LC. The Kinetics of Competitive Radioligand Binding Predicted Mass Action by the Law of Mass Action. *Mol Pharmacol* 1984;25(1):1–9

## **Supplemental Information**

### **Inventory of Supplemental Information**

Appendix S1. Differential equations of models 1 and 2, related to Box 1 and Figure 1. (page 2)

Appendix S2. Approximation and analysis of model 1, related to Figure 3. (page 5)

Appendix S3. Approximation and analysis of model 2, related to Figure 4. (page 10)

Appendix S4. Experimental validation of model 2, related to Figure 4. (page 15)

Appendix S5. Simulation example of local concentrations determining target occupancy, related to Figure 4. (page 17)

Appendix S6. Accuracy of the approximation of model 1, related to Figure 3. (page 19)

Supplemental references. (page 23)

## Appendix S1. Differential equations of models 1 and 2, related to Box 1 and Figure 1.

### Used parameters

$k_{el}$  = first order drug elimination rate constant  
 $k_{in}$  = first order drug distribution rate constant into the tissue  
 $k_{out}$  = first order drug elimination rate constant out of the tissue  
 $k_{off}$  = first order drug-target dissociation rate constant  
 $k_{on}$  = second order drug-target association rate constant  
 $C$  = unbound drug in the central compartment  
 $T$  = unbound drug in the tissue compartment  
 $LR$  = drug-target complex  
 $L_{tot}$  = total drug in de body =  $C + T + LR$   
 $R_{free}$  = unbound target  
 $R_{tot}$  = total target =  $R_{free} + LR$   
[] = concentration  
 $A$  = amount

### Model 1

The rate of change in the amount of drug in the central compartment of model 1,  $AC$ , is given by Equation S1, where  $k_{el}$  and  $k_{off}$  are the first order rate constants describing elimination and drug-target dissociation, respectively, where  $k_{on}$  is the second order drug-target association rate constant,  $[R_{free}]$  is the unbound target concentration and  $ALR$  is the amount of drug-target complex. Drug absorption and non-specific binding are not taken into account.

#### Equation S1

$$\frac{dAC}{dt} = -k_{el} \cdot AC - k_{on} \cdot AC \cdot [R_{free}] + k_{off} \cdot ALR$$

The rate of change of the unbound receptor concentration  $[R_{free}]$ , is given by Equation S2 and the rate of change in the amount of drug-target complex,  $ALR$ , is given by Equation S3

#### Equation S2

$$\frac{d[R_{free}]}{dt} = -k_{on} \cdot [C] \cdot [R_{free}] + k_{off} \cdot [LR]$$

#### Equation S3

$$\frac{dALR}{dt} = k_{on} \cdot AC \cdot [R_{free}] - k_{off} \cdot ALR$$

As the total target concentration is constant in this model,  $[R_{free}]$  can be calculated from the total target concentration  $[R_{tot}]$  and the bound target concentration  $[LR]$  as in Equation S4:

#### Equation S4

$$[R_{free}] = [R_{tot}] - [LR]$$

### Model 2

For model 2, the rate of change in the amount of drug in the central compartment,  $AC$ , is described by Equation S5, where  $k_{out}$  and  $k_{in}$  are the first order rate constants describing distribution into and distribution out of the tissue, respectively, and  $AT$  is the amount of drug in the tissue. Drug absorption and non-specific binding are not taken into account.

**Equation S5**

$$\frac{dAC}{dt} = -k_{el} \cdot AC - k_{in} \cdot AC + k_{out} \cdot AT$$

The rate of change in the amount of drug in the tissue, AT, is described by Equation S6.

**Equation S6**

$$\frac{dAT}{dt} = k_{in} \cdot AC - k_{out} \cdot AT - k_{on} \cdot AT \cdot [R_{free}] + k_{off} \cdot ALR$$

the rate of change of the unbound receptor concentration  $[R_{free}]$ , is given by Equation S7

**Equation S7**

$$\frac{d[R_{free}]}{dt} = -k_{on} \cdot [T] \cdot [R_{free}] + k_{off} \cdot [LR]$$

The rate of change in the amount of drug-target complex in the tissue, ALR, is described by Equation S8.

**Equation S8**

$$\frac{dALR}{dt} = k_{on} \cdot AT \cdot [R_{free}] - k_{off} \cdot ALR$$

The total target concentration is constant in this model, so  $[R_{free}]$  can be calculated from the total target concentration  $[R_{tot}]$  and the bound target concentration  $[LR]$  as in Equation S9:

**Equation S9**

$$[R_{free}] = [R_{tot}] - [LR]$$

All simulations were performed in Berkeley Madonna, version 8.3.18, while visualisations were performed in R, version 3.1.1[1].

## Appendix S2. Approximation and analysis of model 1, related to Figure 1.

As known since the study of Wagner et al[2], the terminal log-linear slope of a PK curve with fast binding equilibrium ( $\lambda_z$ ) is given by Equation S10.

### Equation S10

$$\lambda_z = \frac{k_{el}}{1 + \frac{[R_{tot}]}{K_D}}$$

As explained in box 2, the extensive target binding that leads to a decreased terminal slope of the plasma concentration depends on the ratio of  $[R_{tot}]$  and  $K_D$ . Equation S10 can be derived as in Equation S12 by assuming that the free target concentration equals the total target concentration, since the slope of only the last part of the PK curve is derived. For earlier phases of the PK curve, the target binding might be saturated, leading to a decreased extent of target binding and a steeper PK curve. This saturated part of the PK curve is of interest, as most drugs require a substantial target saturation to be efficacious, especially if the drug is an antagonist.

To make Equation S10 valid for the whole part of the PK curve where equilibrium between bound and unbound drug concentration can be assumed, the value of the target fraction bound (BF) needs to be incorporated as in Equation S13. Here,  $\lambda_{el}(BF)$  describes the derivative of the drug concentration profile over time on semi-log scale (i.e.  $\ln(\text{drug concentration})$  vs. time), as a function of the target fraction bound. This can be derived by recognizing that the total amount of drug decreases with the same rate as the free amount of drug, and by assuming drug-target binding is fast and in equilibrium, as in Equation S12.

### Equation S11

$$BF = \frac{[LR]}{[R_{tot}]}$$

### Equation S12

$$\frac{dAL_{tot}}{dt} = -k_{el} \cdot AL_{tot} \cdot \frac{AC}{AL_{tot}} = -AL_{tot} \cdot \frac{k_{el}}{1 + [R_{tot}] \cdot \frac{1 - BF}{K_D}}$$

### Equation S13

$$\lambda_{el}(BF) = \frac{k_{el}}{1 + [R_{tot}] \cdot \frac{1 - BF}{K_D}}$$

The derivative of the semi-logarithmic drug concentration-time curve,  $\lambda_{el}(BF)$ , is important for the duration of target occupancy, as the rate-limiting (i.e. the slowest) step in the decline of target occupancy can be either the drug-target dissociation or the decline of the free drug concentration.

To calculate the derivative for the semi logarithmic target fraction bound vs. time curve as function of the target fraction bound,  $\lambda_{TO}(BF)$ , it is important to realise that  $\lambda_{el}(BF)$  and  $\lambda_{TO}(BF)$  are equal to each other if elimination is rate limiting in the decline of target occupancy and if the target fraction bound is low. If target binding is saturated (i.e. BF is high), the decline of the unbound target concentration is higher, as explained above and in box 2, but the decline of the bound target fraction is lower. As an example, if the unbound drug concentration decreases 90% from 500 to 50 nM for a drug with a  $K_D$  of 5.0 nM, the corresponding equilibrium bound fraction decreases 7%: from 0.99 to 0.91. If the unbound drug concentration decreases 90% from 50 to 0.50 nM for a drug with a  $K_D$  of 5.0 nM, the corresponding equilibrium bound fraction decreases 82%: from 0.50 to 0.091. To calculate the derivative for the semi-logarithmic target fraction bound vs. time curve if elimination is rate-limiting  $\lambda_{elTO}(BF)$  from  $\lambda_{el}(BF)$ , the relationship between unbound concentration needs to be taken into account. This relationship can be derived from the law of mass action (box 1) as in Equation S14:

**Equation S14**

$$BF = \frac{\frac{L}{K_D}}{1 + \frac{L}{K_D}}$$

As we intend to calculate  $\lambda_{elTO}(BF)$  from  $\lambda_{el}(BF)$ , which are both derivatives on a semi-log scale, we need to obtain the derivative of the logarithm of the BF-unbound concentration relationship, as a function of BF. Thus, we first convert Equation S14 to Equation S15 to obtain the logarithm of BF as function of the logarithm of  $L/K_D$ , which results in Equation S16 after taking the derivative with respect to  $\ln(L/K_D)$ .

**Equation S15**

$$\ln(BF) = \ln\left(\frac{e^{\ln\frac{L}{K_D}}}{1 + e^{\ln\frac{L}{K_D}}}\right)$$

**Equation S16**

$$\frac{d \ln(BF)}{d \ln\left(\frac{L}{K_D}\right)} = \frac{1}{1 + e^{\ln\frac{L}{K_D}}} = \frac{1}{1 + \frac{L}{K_D}}$$

Equation S16 can be rewritten as a function of BF using Equation S14:

**Equation S17**

$$\frac{d \ln(BF)}{d \ln\left(\frac{L}{K_D}\right)} = \frac{1}{1 + \frac{BF}{1 - BF}} = 1 - BF$$

Thus, Equation S18 can be used to obtain  $\lambda_{elTO}(BF)$  from  $\lambda_{el}(BF)$ :

**Equation S18**

$$\lambda_{elTO}(BF) = (1 - BF) \cdot \lambda_{el}(BF) = \frac{(1 - BF) \cdot k_{el}}{1 + [R_{tot}] \cdot \frac{1 - BF}{K_D}}$$

As said before, the decline of the target fraction bound over time can be determined by two processes: dissociation and elimination. Thus,  $\lambda_{elTO}(BF)$  can be compared directly to  $k_{off}$ , which is the slope of the target fraction bound vs. time plot on semi-log scale if drug-target dissociation is rate-limiting in the decline of the target fraction bound.

By selecting the smallest of  $\lambda_{elTO}(BF)$  and  $k_{off}$ , Equation S19 can be used to calculate  $\lambda_{TO}(BF)$ , the slope of the target fraction bound vs. time plot on semi-log scale. In other words, Equation S19 represents our assumption that the decline of target occupancy is determined by the process that gives rise to the slowest decline of target occupancy.

**Equation S19**

$$\lambda_{TO}(BF) = \frac{1}{\frac{1}{\lambda_{elTO}(BF)} + \frac{1}{k_{off}}}$$

To find for what parameter values elimination is the rate-limiting step in the decline of the target fraction bound, Equation S20 can be solved for the parameter of interest.

**Equation S20**

$$\frac{k_{el} \cdot (1 - BF)}{1 + [R_{tot}] \cdot \frac{1 - BF}{K_D}} < k_{off}$$

Equation S20 can be solved for  $k_{on}$  (by rewriting  $K_D$  as  $k_{off}/k_{on}$ , deviding both sides by  $k_{off}$  and rewriting the resultant fraction) to find the required value of  $k_{on}$  to make elimination the rate-limiting step in the decline of the target fraction bound as in Equation S21.

**Equation S21**

$$k_{on} > \frac{k_{el} \cdot (1 - BF) - k_{off}}{[R_{tot}] \cdot (1 - BF)}$$

To obtain from Equation S21 the value of  $k_{on}$  for which elimination is rate-limiting in the decline of BF for all possible values of  $k_{off}$ , it can be reduced to Equation S22 by substituting  $k_{off} = 0$  into Equation S21. Equation S22 equals Equation S23.

**Equation S22**

$$k_{on} > \frac{k_{el} \cdot (1 - BF)}{[R_{tot}] \cdot (1 - BF)}$$

**Equation S23**

$$k_{on} > \frac{k_{el}}{[R_{tot}]}$$

Equation S20 can also be used to find the value of  $k_{off}$  for which elimination becomes the rate-limiting step, for all values of  $k_{on}$ , as it can be reduced to Equation S24 by substituting  $k_{on} = 0$  into Equation S20.

**Equation S24**

$$k_{off} < k_{el} \cdot (1 - BF)$$

Equations 23 and 24 can be rewritten to obtain  $K_{RLon}$  and  $K_{RLOff}(BF)$ , which are the corresponding constants that indicate elimination as rate-limiting step if either  $K_{RLon}$  or  $K_{RLOff}(BF)$  are smaller than 1, as in Equation S25 and S26.

**Equation S25**

$$K_{RLon} = \frac{k_{el}}{k_{on} \cdot [R_{tot}]}$$

**Equation S26**

$$K_{RLOff}(BF) = \frac{k_{el} \cdot (1 - BF)}{k_{off}}$$

The  $k_{off}$  value that marks the transition where the slope of target occupancy for a rate-limiting elimination ( $\lambda_{elTO}(BF)$ ) starts to be strongly influenced by the affinity can be derived from Equation S18 and is given by Equation S27, which can be rewritten as Equation S28.

**Equation S27**

$$\frac{[R_{tot}] \cdot (1 - BF)}{K_D} = 1$$

**Equation S28**

$$k_{off} = [R_{tot}] \cdot (1 - BF) \cdot k_{on}$$

The threshold values as obtained in equations 25, 26 and 28 provide the relation of Figure 3 with all the parameters of model 1 that are not explicitly incorporated in Figure 3:  $[R_{tot}]$ ,  $BF$  and  $k_{el}$ .



### Appendix S3. Approximation and analysis of model 2, related to Figure 4.

Since model 2 is similar to model 1, the prediction of the derivative of the target fraction bound ( $\lambda_{TO}(BF)$ ) over time as function of the target fraction bound (BF) for model 2 has similar components as for model 1. Since model 2 has three compartments, three processes can be rate-limiting for the decrease of the target fraction bound; drug-target dissociation, unbound drug distribution and unbound drug elimination. If drug-target dissociation is rate limiting,  $\lambda_{TO}(BF)$  is equal to  $k_{off}$ . If the unbound drug distribution from tissue to plasma is rate limiting, the distribution is influenced by drug-target binding in a similar way as the elimination is influenced by drug-target binding (see Equation S13) for model 1. The resultant derivative for the unbound concentration in tissue vs time curve on semi logarithmic scale, as function of the target fraction bound,  $\lambda_{out}(BF)$ , is thus given by Equation S29.

#### Equation S29

$$\lambda_{out}(BF) = \frac{k_{out}}{1 + [R_{tot}] \cdot \frac{1 - BF}{K_D}}$$

If the unbound drug elimination is rate limiting, the derivative for the unbound concentration in the blood vs time curve on semi logarithmic scale, as function of the target fraction bound,  $\lambda_{el}(BF)$  is influenced again by the fraction of the drug that resides in the central compartment. This fraction is for model 2 not only determined by the drug target binding, but also by the tissue distribution. If passive diffusion is assumed to be the only mechanism of drug distribution, leading to equal equilibrium concentrations in both tissue and plasma, the ratio of the amount of drug in the central compartment (AC) and the total amount of drug in the body ( $L_{tot}$ ) in equilibrium is given by Equation S30, which can be rewritten as Equation S31.

#### Equation S30

$$\frac{AC}{AL_{tot}} = \frac{V_C}{V_C + V_T + V_T \cdot \frac{[LR]}{[T]}}$$

#### Equation S31

$$\frac{AC}{AL_{tot}} = \frac{V_C}{V_C + V_T \cdot \left(1 + [R_{tot}] \cdot \frac{1 - BF}{K_D}\right)}$$

With the ratio of amounts of drug in the central compartment and in the total body as in Equation S31,  $\lambda_{el}(BF)$  is given by Equation S32.

#### Equation S32

$$\lambda_{el}(BF) = k_{el} \cdot \frac{V_C}{V_C + V_T \cdot \left(1 + [R_{tot}] \cdot \frac{1 - BF}{K_D}\right)}$$

As  $\lambda_{out}(BF)$  and  $\lambda_{el}(BF)$  represent the derivatives of the unbound drug concentration vs time profile on semi logarithmic scale, Equation S17 can be used to get the corresponding derivatives of the bound drug concentration vs time profile on semi logarithmic scale, as in equations 33 and 34.

With the values of  $k_{off}$ ,  $\lambda_{outTO}(BF)$  and  $\lambda_{elTO}(BF)$ , the derivative of the target fraction bound vs. time on semi logarithmic scale can be approximated according to Equation S35.

#### Equation S33

$$\lambda_{outTO}(BF) = \cdot \frac{k_{out} \cdot (1 - BF)}{1 + [R_{tot}] \cdot \frac{1 - BF}{K_D}}$$

Equation S34

$$\lambda_{elTO}(BF) = k_{el} \cdot (1 - BF) \cdot \frac{V_C}{V_C + V_T \cdot \left(1 + [R_{tot}] \cdot \frac{1 - BF}{K_D}\right)}$$

Equation S35

$$\lambda_{TO}(BF) = \frac{1}{\frac{1}{\lambda_{elTO}(BF)} + \frac{1}{\lambda_{outTO}(BF)} + \frac{1}{k_{off}}}$$

Equation S35 can be used to identify the rate-limiting step in the decline of the target fraction bound similarly as Equation S19, but the dependency on the parameters is more complex as there are three possible rate-limiting steps. To find the maximal  $k_{on}$  value for which drug-target dissociation is the rate limiting step in the decline of the target fraction bound, either  $\lambda_{outTO}(BF)$  or  $\lambda_{elTO}(BF)$  needs to be smaller than  $k_{off}$ , as described by Equation S36.

Equation S36

$$\frac{k_{el} \cdot (1 - BF) \cdot V_C}{V_C + V_T \cdot \left(1 + [R_{tot}] \cdot \frac{1 - BF}{K_D}\right)} < k_{off} \text{ or } \frac{k_{out} \cdot (1 - BF)}{1 + [R_{tot}] \cdot \frac{1 - BF}{K_D}} < k_{off}$$

This equation is solved in the same way as Equation S20 to obtain the minimal value of  $k_{on}$  for which no value of  $k_{off}$  results in dissociation as the rate-limiting step in the decrease of the target fraction bound, which gives Equation S37. Equation S37 comprises two components as well, which can be rewritten to two more simple equations as in Equation S38 and Equation S39 where  $\min\{\}$  is an operation that selects the minimal value of its input values.

Equation S37

$$k_{on} > \frac{k_{el} \cdot \frac{V_C}{V_T}}{[R_{tot}]} \text{ or } k_{on} > \frac{k_{out}}{[R_{tot}]}$$

Equation S38

$$k_{on} > \frac{k_{minon}}{[R_{tot}]}$$

Equation S39

$$k_{minon} = \min\left\{k_{el} \cdot \frac{V_C}{V_T}, k_{out}\right\}$$

Equation S36 can also be used to find the minimal value of  $k_{off}$  for which no values of  $k_{on}$  result in dissociation as the rate-limiting step in the decline of the target fraction bound in a similar way as Equation S20 by substituting  $k_{on} = 0$  into Equation S36. As a result, Equation S40 is obtained. The value of  $k_{off}$  for which dissociation is not rate-limiting for all values of  $k_{on}$  is given by Equation S41 and S42.

**Equation S40**

$$k_{off} > k_{el} \cdot (1 - BF) \cdot \frac{V_C}{V_C + V_T} \text{ or } k_{off} > k_{out} \cdot (1 - BF)$$

**Equation S41**

$$k_{off} = k_{minoff}$$

**Equation S42**

$$k_{minoff} = \min \left\{ k_{el} \cdot (1 - BF) \cdot \frac{V_C}{V_C + V_T}, k_{out} \cdot (1 - BF) \right\}$$

The  $k_{off}$  value that marks the transition where the decline of occupancy for a rate-limiting elimination ( $\lambda_{elTO}(BF)$ ) or rate-limiting distribution ( $\lambda_{outTO}(BF)$ ) starts to be strongly influenced by the affinity can be derived from Equation S33 and S34 and is given by Equation S43 for  $\lambda_{elTO}(BF)$  and Equation S44 for  $\lambda_{outTO}(BF)$ .

**Equation S43**

$$\frac{V_T \cdot [R_{tot}] \cdot (1 - BF)}{K_D} = V_C + V_T$$

**Equation S44**

$$\frac{[R_{tot}] \cdot (1 - BF)}{K_D} = 1$$

Equations 43 and 44 can be rewritten as Equation S45 and S46, respectively

**Equation S45**

$$k_{off} = \frac{V_C + V_T}{V_T} \cdot k_{on} \cdot [R_{tot}] \cdot (1 - BF)$$

**Equation S46**

$$k_{off} = k_{on} \cdot [R_{tot}] \cdot (1 - BF)$$

S45 and 46 can be summarized by Equation S47.

**Equation S47**

$$k_{off} = \frac{k_{minoff}}{k_{minon}} \cdot k_{on} \cdot [R_{tot}]$$

#### Appendix S4. Experimental validation of model 2, related to Figure 4.

Model 2 was fitted to describe digitised literature summary data of [<sup>3</sup>H]diprenorphine brain and serum concentrations [3] with NONMEM version 7.3, ADVAN6 [4]. The results of our model fit and the obtained literature data are plotted in Figure S1, and the estimated parameter values are given in table S1.

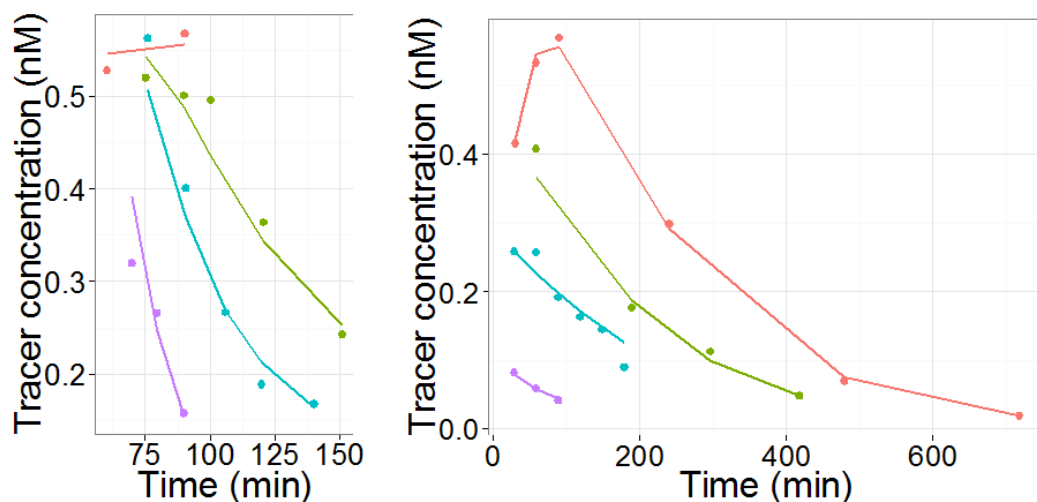
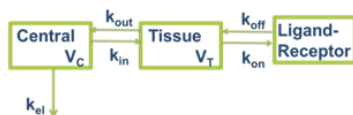


Figure S1. NONMEM fits of model 2 (lines) of [<sup>3</sup>H] diprenorphine brain radioactivity data after administration of a tracer and unlabeled dose of diprenorphine as obtained from Perry et al. (points) [3]. Unlabeled diprenorphine was administered at  $t=60$  min (left panel) or at  $t=0$  (right panel) at different doses: 0 (red), 24 (green), 50 (blue), 500 (purple) nmol/kg. The tracer dose was 0.10 nmol Top: model structure of model 2, which was used to fit these data.

Table S1. Parameter estimates for [<sup>3</sup>H]diprenorphine. Proportional errors were 0.6% and 9% with uncertainties of 29% and 19% in plasma and brain, respectively.

Parameter	Estimate (% CV)
$k_{el}$ ( $h^{-1}$ )	0.96 (0.6)
$k_{in}$ ( $h^{-1}$ )	0.29 (4.1)
$k_{out}$ ( $h^{-1}$ )	17 (5.5)
$k_{on}$ ( $nM^{-1}h^{-1}$ )	5.6 (4.7)
$k_{off}$ ( $h^{-1}$ )	4.0 (3.8)
[R <sub>tot</sub> ] (nM)	20 (4.0)
$V_C$ (L)	2.9 (0.6)
$V_T$ (L)	0.022 (4.0)

**Appendix S5. Simulation example of local concentrations determining target occupancy, related to Figure 4.**

To simulate the relative impact of  $k_{on}$  and  $k_{off}$  in a relevant set of parameters, obtained from *in vivo* measurements, we used the parameter values as obtained from fitting model 2 to literature diprenorphine data (see appendix S5). In these simulations, either  $k_{on}$  or  $k_{off}$  were changed which means that the  $K_D$  changed accordingly. To compensate the effect of a changing  $K_D$  on the extent of target binding in equilibrium and to obtain relevant target occupancies, the dose was normalized for the  $K_D$ . On basis of our approximations, we would expect a similar impact of  $k_{on}$  and  $k_{off}$  on the duration of target occupancy for these parameter values, which was confirmed by our simulations, see Figure S2. These simulations also demonstrate clearly that only the local (i.e. brain) free drug concentrations are affected by drug-target binding, while the plasma free drug concentrations remain mainly unaffected (Figure S2).

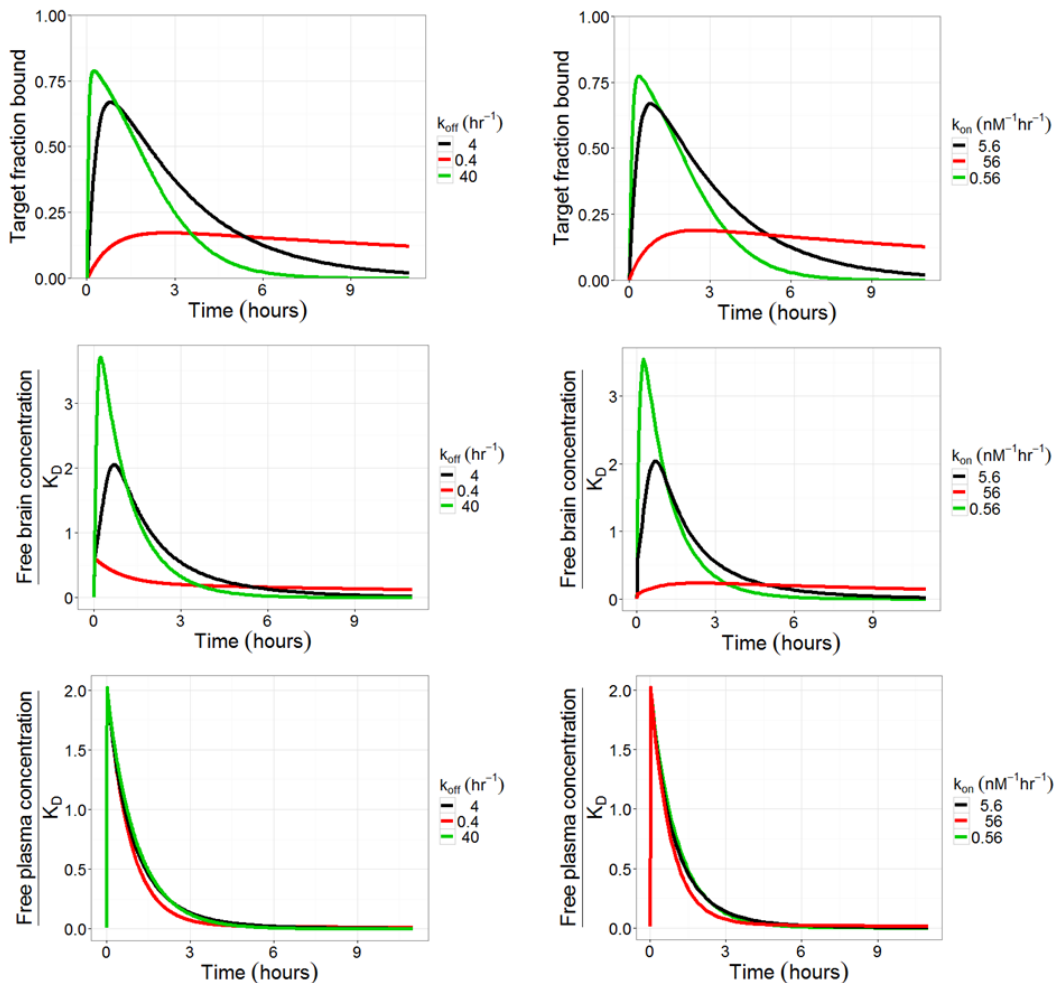


Figure S2. Simulated target binding of diprenorphine (black lines) and 2 hypothetical drugs (red and green lines) with a 10-fold decrease and increase in  $k_{off}$  (left-hand panels) or  $k_{on}$  (right-hand panels). The other parameter values remain constant:  $k_{el} = 0.96$ ,  $k_{in} = 0.29$ ,  $k_{out} = 17$ ,  $V_c = 2.9$  L,  $V_T = 0.022$  L. The dose was normalised for the affinity:  $dose = K_D * 5.9$  nmol.

### Appendix S6. Accuracy of the approximation of model 1, related to Figure 3.

To identify the accuracy of our approximation of the derivative of the semi logarithmic target occupancy curve, simulation studies (“observed slope”) were compared with the results of the approximation, the “approximated slope” for different target concentrations, dissociation and elimination rate constants. To obtain a normalized measure for the accuracy of our approximation, we used the ratio of the approximated and simulated slope, which equals 1 for a perfect approximation. First, we analysed the accuracy over time for a regular set of pharmacokinetic and binding kinetic parameters, with a low target concentration, see Figure S3. The initial phase of the target occupancy is not predicted accurately for the simulation with a low  $k_{off}$  value as the time to reach maximum target occupancy is increased by a low  $k_{off}$ , and our approximation is only meant for the decreasing phase of the target occupancy profile. This initial phase is longer for combinations of low  $k_{off}$ ,  $k_{on} \cdot [R_{tot}]$  and  $k_{el}$ . This can be seen in Figure S4, where a low elimination rate (0.1/hr) constant leads to inaccurate predictions at 24 hours post dosing for low target concentrations, compared to a high elimination rate constant(1/hr). This inaccuracy is still only present for the low target concentrations if the elimination rate constant is further decreased to an extremely low value (0.001/hr), see Figure S5. Furthermore, our approximation can introduce a underestimation of the derivative of the semi logarithmic target fraction bound vs time curve of up to two fold. This underestimation is especially observed for low target concentrations.

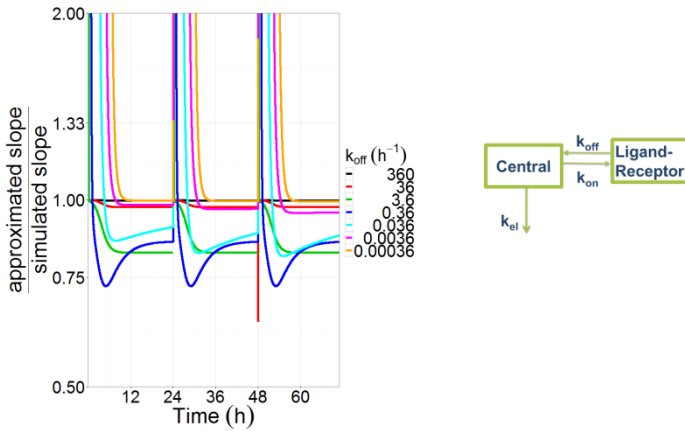


Figure S3. Simulations with model 1 for the time-dependent accuracy of Equation S19 for various values of  $k_{off}$  after repeated dosing.  $k_{el} = 1/hr$ ,  $k_{on} = 0.36/(nM*hr)$ ,  $[R_{tot}] = 1nM$

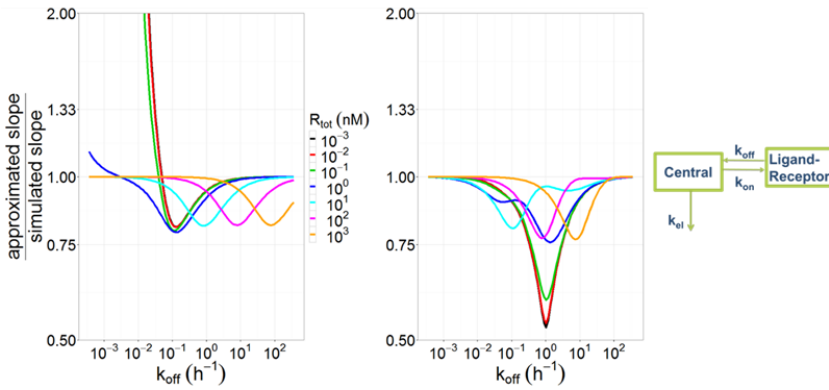


Figure S4. The accuracy of equation S19 for model 1 at 24 hours post dosing depends on the value of  $k_{off}$ ,  $[R_{tot}]$  and  $k_{el}$ .  $k_{el} = 0.1/hr$  (left panel) and  $1/hr$  (right panel),  $k_{on} = 0.36/(nM*hr)$ .

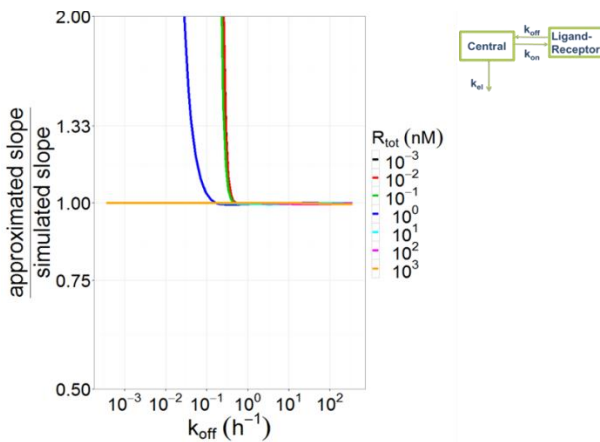


Figure S5. The accuracy of Equation S19 for model 1 at 24 hours post dosing depends on the value of  $k_{off}$ ,  $[R_{tot}]$  and  $k_{el}$ .  $k_{el} = 0.001/hr$ ,  $k_{on} = 0.36/(nM*hr)$ .

## Supplemental References

1. R Core Team. R: A language and environment for statistical computing. R Found Stat Comput Vienna, Austria URL <http://wwwR-project.org/> 2013;
2. Wagner JG. A new generalized nonlinear pharmacokinetic model and its implications. In: Wagner JG, editor. Biopharmaceutics and Relevant Pharmacokinetics Hamilton, IL; 1971. p. 302–17
3. Perry DC, Mullis KB, Oie S, et al. Opiate antagonist receptor binding in vivo: evidence for a new receptor binding model. *Brain Res* 1980;199(1):49–61
4. Beal S, Sheiner LB, Boeckmann A, et al. NONMEM 7.3.0 Users Guides. (1989-2013). Icon Development Solutions